



Ka-Band signal propagation experiment at NESAC Umiam

Anjan Debnath*

North Eastern Space Applications Centre, Umiam, Meghalaya 793103, India.

Received 13 November 2017

A Ka-Band signal propagation study under tropical monsoon climate has been taken up jointly by ISRO/ONERA/CNES. The program has been aimed at finding the degree to which Ka-Band satellite signals get affected by rain. Dual polarized Ka Band beacon signals onboard GSAT-14 satellite, of frequencies 20.2 GHz and 30.5 GHz, have been used for the experiment. Data available by various instruments has been compared with ITU-R predicted values. Results for the years 2016 and 2017 at Umiam has shown underestimation of both Rainfall and Signal Attenuation by ITU-R predicted models. It has also been found that the Rainfall has been mostly concentrated in three months (June, July, August) and the maximum attenuation that Ka-Band signals have suffered during rain at Umiam has been around 30-40 dB. The actual Rainfall and Attenuation of both 20.2 GHz and 30.5 GHz signals have been compared with ITU-R predictions and has been found to be much above the predicted levels. A Study of the Z-R relationship for the rainfall and comparison with known relations has indicated that a new distribution is required for the region.

Keywords: Ka-Band, Beacon receiver, Laser precipitation monitor, Rain rate, Z-R relationship

1 Introduction

Satellite communication (satcom) has seen an unforeseen growth in the recent years with other modes of wireless communication (i.e., cellular mobile communication) seeming to have reached their saturation levels and have been suffering from various limitations, answers to which has been known to satellite communication industry. This, along with the fact that satcom has reached the level of maturity where user equipments have been smaller, compact and affordable; communication protocols have been standardized (DVB-S2, DVB-RCS, DVB-T etc.) and sufficient resource allocation has been promised by launching multitude of satellites, requires that newer satellite frequency bands (other than the saturating C and Ku Bands) be explored in more detail.

The satellite frequency band mostly used in India is C band, because C band signals (4GHz to 8 GHz, satellite uplink/ downlink band of 6GHz/ 4 GHz), has been generally interference prone from other microwave links and user receiving terminals operating in these frequency band has been bigger in size (dish antennas of 1.8 or 2.4 meter diameter) and expensive. While Ku band frequencies has been relatively less interference prone and user equipments have been smaller (dishes with sub-meter diameter)

and low- priced, the satellite bandwidth itself has been costlier and prone to high rain fade. But still, the rain fade at Ku band has been much lower compared to Ka-Band (downlink of Ka-Band suffers 3 to 10 times more than Ku-Band in high rainfall and uplink of Ka-Band suffers 63-400 times more than Ku-Band). Apart from rain attenuation, there has been other impairments to Ka-Band signal, like gaseous absorption, cloud attenuation, rain and ice depolarization and tropospheric scintillation, all mainly due to the smaller wavelength of the signal, which has been comparable to hydrometers (rain, ice, snow, hail etc.).

Also, because the Ka-Band receiving equipment has been smaller in size, these cannot produce much gain or output power to compensate for absorptive signal losses. Therefore, the standards of satcom (DVB-S2 and DVB-RCS) have incorporated in them fade mitigation techniques^{1,2} which adapt technical parameters of the system according to the propagation problem.

2 Objective

In numerous technical reports, studies of rain attenuation of microwave signals for varying periods have been mentioned. It was clear from early reports that there is a relationship of signal power attenuation with the rain rate but for a long time, no uniform model could be put forward that can work for different climate zones. It was found that in temperate

*Corresponding Author: (E mail: anjan.debnath@nesac.gov.in)

climate, signals above 10 GHz suffer rain attenuation but in tropical regions where the raindrops are generally bigger, the impact of rain attenuation starts becoming prominent for signals as low as 7 GHz.³ The European countries where rainfall is generally less than tropical regions, are better suited to use the Ka-Band. This has, for some time, checked the progress of system design for Ka-Band satellite systems in tropical regions. The figure given below shows the coverage of Ka-Band commercial use in the World at present. It was primarily the motivation behind the study to understand how much Ka-Band signal may get attenuated at worst cases so that satellite links may be designed with sufficient margin.

3 Theoretical background

For modelling of rain attenuation, various terminologies are used. They are given briefly here for ready reference.

Rainfall Intensity, which is found to be in some relationship with the value of signal power attenuated over the rain free attenuation level, is quantified through the *rain rate*, which is measured in the units of mm/h. To represent the variability of rainfall intensity with time, a *complementary cumulative distribution function (CCDF)* is used which gives the percentage of time of any year (p%) exceeded for which a certain threshold rainfall rate (R_p mm/h) has been recorded. Therefore, if for a place, $R_{0.01} = 30$ mm/h, it means that on average, for 0.01% of time of one year (about 53 minutes), the rainfall rate exceeds 30 mm/h and otherwise it stays lower.

Specific Attenuation and Effective Rainy Path Length

It is generally assumed that the signal power attenuation (A , in dB) over the effective rainy path length for a point rainfall rate is given by the following simplified power law equation

$$A(\text{dB}) = kR^\alpha L_{\text{eff}}(1)^4$$

where, the part kR^α is called specific attenuation (units of dB/km) and L_{eff} is the effective Rainy Path Length,

through which uniform attenuation of signal has occurred. k and α are frequency and polarization dependent coefficients.

Though sounding experiments during rain has revealed varying rain intensity at different tropospheric heights, it is assumed in this simplified model that rain intensity is constant vertically and the microwave signal travels through a homogenous media consisting of suspended spherical rain particles in a slant path which starts from the theoretical freezing height in the troposphere (H_f) at which Rain starts and terminates at the rain receiving point on the ground (H_r). It is also assumed that the rainfall can be described by a point rainfall rate.⁵

4 Experimental setup

The experiment used a system of two Satellite Beacon Receivers, procured by ONERA, France which measured the GSAT-14 Ka-Band beacons at 20.2 GHz and 30.5 GHz. The main technical parameters of the experiment are detailed in Table 1 and its six ground stations' data are given in Table 1.

4.1 Instrument description

NESAC, Umiam, is located in a hilly region with wet tropical climate. Mostly the rainfall occurs during June-September but May and October also show some rainfall. The experimental setup comprises of several meteorological instruments collocated with the satellite receiver.

Tipping bucket type rain gauge: This instrument allows measurement of rain intensity with 1-min integration time. This rain gauge collects the time of each tip so that for each interval between two consecutive tips, 'instantaneous' rainfall rate can be calculated as the ratio of the rain amount in one tip, or bucket size, which corresponds to 0.1 mm, to the time between tips in seconds. An integration time of 1-minute is then applied to derive rainfall rate from the aforementioned values.

Also, a micro rain radar (MRR-2; METEK) and a (LPM), are available. These equipments can get

Table 1 — Satellite & Earth Station technical data of GAT-14 Experiment at NESAC

Satellite name and orbital position	GSAT-14 (74°E)
Beacon transmit frequency	20.2 GHz and 30.5 GHz
Equivalent Isotropic Radiated Power 24 dBW	
Frequency Stability (Over operating temperature)	±1.0 ppm
Receive Station Name	NESAC, Umiam
Geographic Location	25.67° N, 91.91° E, 1038 mtr above MSL
Receiver Station to Satellite Elevation Angle	53.95°

vertical profiles of rain which include rain drop size distribution (**RDS**) and rain intensity profiles. Apart from all these, an atmospheric humidity profiling radiometer (RPG-HumproG4) is also installed for calibration of receivers. This has seven scan channels from 22.24 GHz to 31.84 GHz and an inbuilt micro weather station. Their basic technical parameters are stated in Table 2.

4.2 Rain attenuation determination

Signal Attenuation caused due only to rain absorption and scattering losses can be calculated from a measurement of received satellite-emitted signal power at the Beacon receiver antenna input with a prior idea regarding average signal attenuation in non-rainy condition.

To get this knowledge, the following method has been adopted. The beacon receiver data has been categorized into rainy and non-rainy types with the help of ‘Rain Flag’ value present in the data files. When the flag is set, it indicates rainy condition and vice versa. Every time the rain flag is set for a sufficient duration, indicating a spell of rain, using this ‘Rain Flag’, easily two reference points can be taken to be before the start of rain event and after its end. Rainy spells of duration more than one hour has

also been seen to include zero rain attenuation intervals. The received power levels at these non-rainy but close to rain event points represent an estimation of cloud attenuation and attenuation due to water vapour.

This non-rainy power level can be subtracted from rainy power levels for the corresponding rain event to get the corresponding rain attenuation only.

4.3 Rain rate and attenuation variation over observation period

From the day of installation of equipment (24 February 2016) to 31 December 2016, a total of 130 days’ data for all the equipment are available. Of these, 31 are Rainy Days and 99 are Non-Rainy days.

The data availability has been affected by site specific logistic difficulties and power problems.

4.3.1 ITU- R prediction method

The ITU-R method described in ITU-R Recommendation P. 837-7⁷ has been followed to determine Monthly Rainfall probability according to following formula:

$$P_{0ii} = 100 \times \frac{MT_{ii}}{24 \times N_{ii} \times r_{ii}} (\%) \dots(1)$$

Where, ii is the number of month, N_{ii} is the average days in month ii, MT_{ii} is monthly mean total rainfall (mm), The obtained values are tabulated in Table 3.

Table 3 - Determination of parameters of ITU-R model for prediction of annual rainfall probability (as per table format given in⁷).

Finally, calculation of annual probability of rain $P_{0annual} = P(R>0)$ is done according to formula (2).

$$P_{0annual} = \frac{\sum_{ii=1}^{12} N_{ii} \times P_{0ii}}{365.25} \dots(2)$$

And it was found that, $P_{0annual} = 6.6521 \%$

Table 2 — Technical Parameters of Meteorological Instrument at NESAC, Umiam

Equipment & Specification	Value
	Tipping bucket rain gauge
Make	Teledyne
Bucket size	0.01 mm
	Laser precipitation monitor
Make & model	ThiesClima
Laser beam wavelength	785 nm(Infrared)
Measuring area	7 sq. Inch(465 sq. Mtr.)
Minimum intensity	0.005 mm/h (drizzle)
	Humidity profiler radiometer (RPG-HUMPRO) ⁶
Number of channels	07 (Filter Bank)
Channel centre frequencies	22.24 GHz, 23.04 GHz, 23.84 GHz,25.44 GHz, 26.24GHz, 27.84 GHz, 31.4 GHz (K-Band)
Channel bandwidth	230 MHz all frequencies

Table 3 — Determination of parameters of ITU-R model for prediction of annual rainfall probability (as per table format given in⁷)

Month	Jan	Feb	Mar	Apr	May	Jun	Jul	Aug	Sep	Oct	Nov	Dec
ii	01	02	03	04	05	06	07	08	09	10	11	12
N_{ii}	31	28.25	31	30	31	30	31	31	30	31	30	31
$MT_{ii}(mm)$	13.57	23.67	63.27	149.29	396.44	782.64	662.94	477.05	390.13	217.58	31.48	6.81
$r_{ii}(C)$	2.3310	2.9043	4.0372	4.6827	5.1650	5.8498	5.9750	6.1246	5.7474	5.0344	3.6797	2.6612
$P_{0ii}(\%)$	0.783	1.202	2.106	4.4279	10.317	18.582	14.913	10.469	9.428	5.809	1.188	0.344

Now, following the method, we determine rain rate for different percentage exceedence. The values are mentioned in Table 4.

4.3.2 Monthly rainfall analysis

With the state of the art Thies clima laser precipitation monitor, we can easily obtain 2016 (Fig. 1).

A complementary cumulative distribution function of the one minute integrated rainfall rate obtained from the data of rain gauge instrument, for rain

statistics for individual months and days, even for hours also. A plot showing the actual rainfall statistics (CCDF) at Umiam for the period from May 2017 to September, 2017 from the LPM and ITU-R predicted rainfall for average year are shown in Fig. 2 for comparative analysis.

4.3.3 Z-R relationship for rain

Table 5 shows the observed a and b coefficients of the power law Z-R relationship, observed from

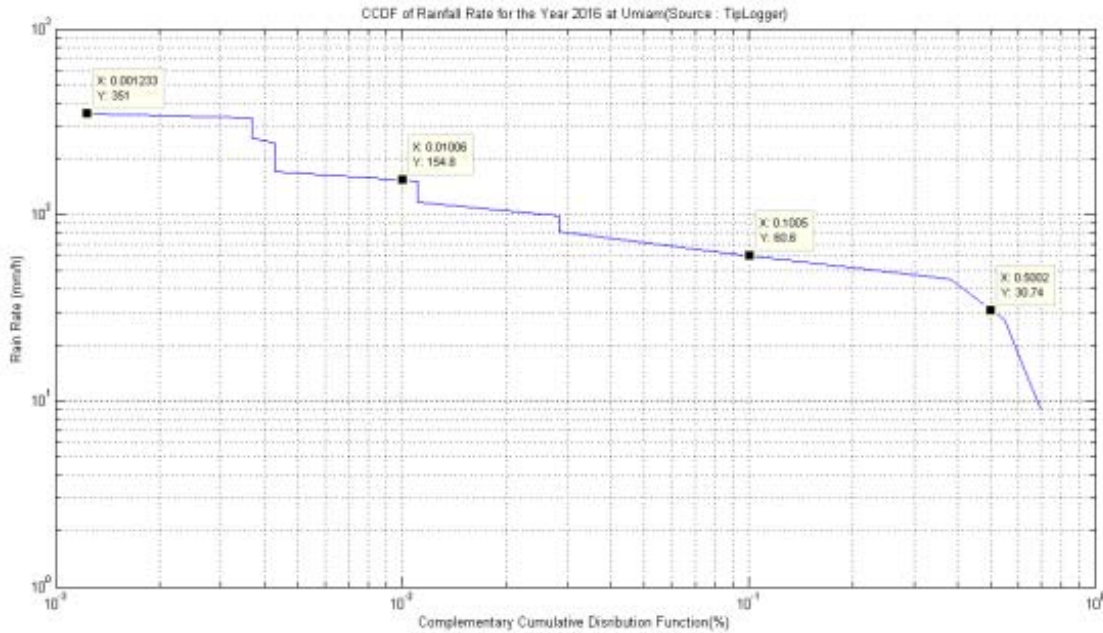


Fig. 1 — CCDF of rainfall intensity

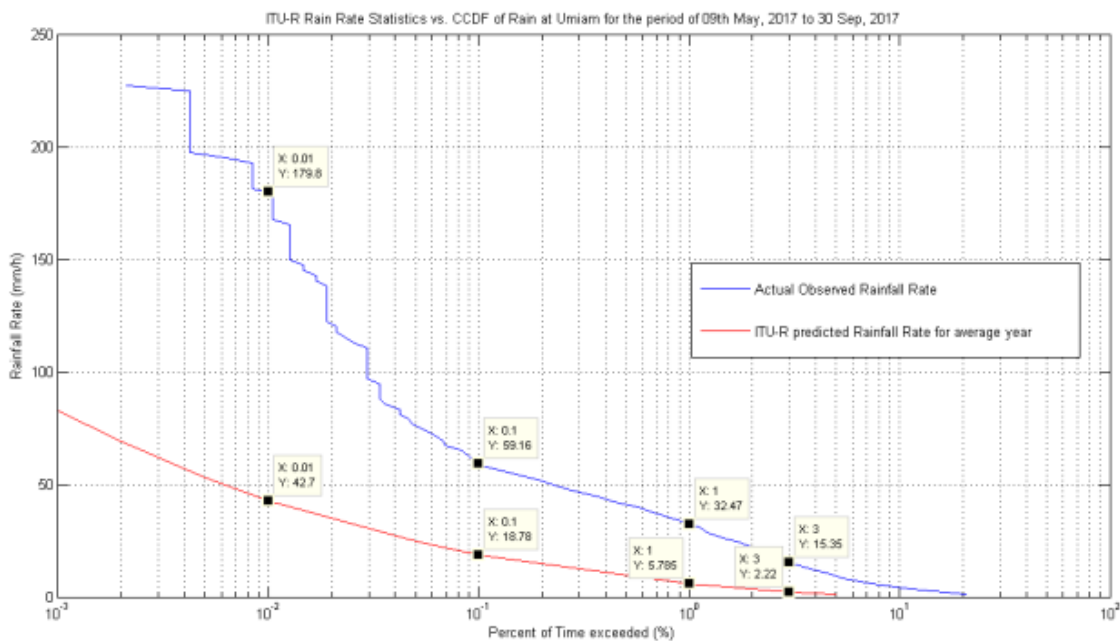


Fig. 2 — ITU-R predicted Rainfall vs. Actual Rainfall statistics at Umiam (2017)

the LPM for the months May to September, 2017.

4.3.4 Rainfall attenuation statistics

A comparative plot was made to describe the attenuation values for 20.2 GHz and 30.5 GHz beacon signals with ITU-R predicted attenuation for 20.2 GHz signal⁸. Figure 3 shows the plot:

5 Discussion

From the Rainfall Statistics predicted by ITU-R and obtained from actual observations, following table can be prepared. Here, deviations (%) of ITU-R prediction from actual observations have been calculated according to following formula:

$$\text{Deviation (\%)} = \frac{(\text{Actual Observation} - \text{ITU-Prediction})}{(\text{Actual Prediction})} \times 100 \quad \dots (3)$$

Table 4 — Rain Rate for different percentage exceedence obtained from ITU-R prediction model

Percentage(%)	5	1	0.1	0.01	0.001
R (mm/h)	0.95	5.78	18.78	42.7	83

Table 5 — Observed values of parameters of Z-R relationship from LPM(May, 2017 to September, 2017)

Month	Observed a,b values
May	a=139, b= 1.2
June	a=170.68, b=1.324
July	a=161.867, b=1.367
August	a=181.559, b=1.354
September	a=179.39, b=1.342

Obtained results have been tabulated in Table 6.

So, it is very clear that actual rainfall at Umiam is very much underestimated in ITU-R model. Similar comparison for the individual months also is shown in Table 7.

Also, the Z-R relationship analysis reveals that the monthly Z-R relationships do not match well with existing common Z-R models, like Marshall-Palmer⁹, WSR-88D¹⁰ Convective or Rosenfeld Tropical¹¹ model. The deviation of the model parameters (a,b) from the actual observed (a,b) is tabulated below in Table 8. The deviations (Δa , Δb) are determined according to the formula 4.

$$\Delta a = \frac{(\text{Actual value of a} - \text{model value of a})}{\text{actual value of a}} \times 100$$

$$\Delta b = \frac{(\text{Actual value of b} - \text{model value of b})}{\text{actual value of b}} \times 100 \quad \dots(4)$$

From the table, it can be seen that only West-Cool Stratiform and East-Cool Stratiform models

Table 6 — Deviation between actual and ITU-R predicted rainfall rate at different percentage exceedence

Rainfall exceedence Percentage (%)	1.0	($\Delta 1$)	0.1	($\Delta 0.1$)	0.01	($\Delta 0.01$)
ITU-R prediction	5.785	0	18.78	0	42.7	0
Actual observation- 2016	30.74	81.18	60.6	69	154.8	72.41
Actual observation- 2017	32.47	82.18	59.16	68.25	179.8	76.25

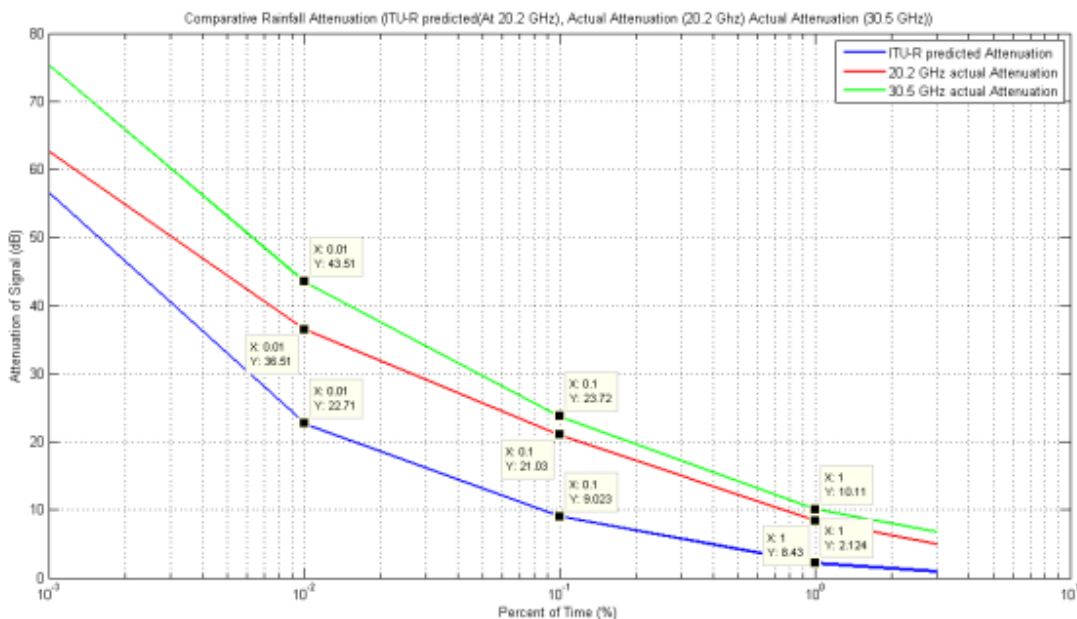


Fig. 3 — Comparative analysis of rainfall attenuation for Umiam, ITU-R predicted Attenuation vs. Actual attenuation (20.2 GHz and 30.5 GHz)

Table 7 — Rainfall Rates for different percentage Exceedence for different months of 2017

Month, Year	$R_{0.01}$ (mm/h)	$R_{0.1}$ (mm/h)	$R_{1.0}$ (mm/h)	$R_{3.0}$ (mm/h)	$R_{10.0}$ (mm/h)
May, 2017	Data inadequate	Data inadequate	Data inadequate	Data inadequate	Data inadequate
June, 2017	117.3	75.44	32.6	17.9	6.03
July, 2017	58.37	50.78	26.79	11.8	2.73
August, 2017	Data inadequate	Data inadequate	44.7	25.98	7.37
September, 2017	Data inadequate	143.4	35.55	17.7	4.92

Table 8 — Deviation of observed parameters from common models

Month	Marshall-Palmer ($a=200, b=1.6$)(%) (after ⁹)	WSR-88D convective ($a=300, b=1.4$)(%) (after ¹⁰)	Rosenfeld tropical ($a=250, b=1.2$)(%) (after ¹¹)
May	$\Delta a = -43.88, \Delta b = -33.33$	$\Delta a = -115.83, \Delta b = -16.66$	$\Delta a = -79.86, \Delta b = 0$
June	$\Delta a = -17.18, \Delta b = -20.85$	$\Delta a = -75.77, \Delta b = -5.74$	$\Delta a = -46.47, \Delta b = 9.36$
July	$\Delta a = -23.56, \Delta b = -17.04$	$\Delta a = -85.33, \Delta b = -2.41$	$\Delta a = -54.75, \Delta b = 12.21$
August	$\Delta a = -10.16, \Delta b = -18.17$	$\Delta a = -65.23, \Delta b = -3.4$	$\Delta a = -37.69, \Delta b = 11.37$
September	$\Delta a = -11.49, \Delta b = -19.23$	$\Delta a = -67.23, \Delta b = -4.32$	$\Delta a = -39.36, \Delta b = 10.58$
Mean	$ \Delta a = -21.25, \Delta b = -21.72$	$ \Delta a = -69.2, \Delta b = -6.51$	$ \Delta a = -51.63, \Delta b = -8.7$

underestimate the parameter a while others overestimate it.

The Marshall-Palmer parameter a is the closest to observed value of a (21.25% overestimation). Similarly, the WSR-88D model parameter b is the closest to observed value of b (6.5% overestimation). Therefore, it can be said that a new Z-R equation may be needed.

References

- ETSI EN 302 307-1 v1.4.1 (2014-11). Digital Video Broadcasting (DVB); Second generation framing structure, channel coding and modulation systems for Broadcasting, Interactive Services, News Gathering and other broadband satellite applications.
- ETSI EN 301 790 v1.5.1(2009-05). Digital Video Broadcasting (DVB); Interaction channel for Satellite Distribution System.
- Moupfouma F & Tiffon J, *IET Electronics Letters*, 18 (1982) 1012.
- Olsen R L, Rogers D V & Hodge D B, *IEEE Transactions of Antennas & Propagation*, 26 (1978) 318.
- International Radio Consultative Committee(CCIR), vol. V, Rep. 721-1 XVth Planetary Assembly, Geneva, 1983.
- RPG Technical Instrument Manual, RPG-MWR-STD-TM, Issue 01/02, 20, 29.09.2013.
- ITU-R Recommendation 837-6(02-2012), Characteristics of Precipitation for Propagation Modelling.
- ITU-R Recommendation, Propagation data and prediction methods required for the design of Earth-space telecommunication systems, 10 2009.
- Marshall J S and Palmer W M, *Journal of Meteorology*, 5 (1948) 165.
- Fulton R A, Breidenbach J P, Seo D-J, Millerand D A, O'Bannon T, *Weather Forecasting*, 13 (1998) 388.
- Rosenfeld D, Wolff DB, & Atlas D, *Journal of Applied Meteorology*, 32 (1) (1993) 50.